A New Hybrid Particle Scheme Using Electromagnetic Fields

L. Chen[1,2] Y. Lin[3], X, Y. Wang[3], and J, Bao[4]

[1]Institute for Fusion Theory and Simulation and Department of Physics, Zhejiang University, Hangzhou, China

[2]Department of Physics and Astronomy, University of California Irvine, Irvine, CA, USA.

[3]Physics Department, Auburn University, Auburn, AL 36849, USA.

[4]Fusion Simulation Center, Peking University, Beijing, China.

July 2018

Abstract. We have developed a new gyrokinetic electron and fully kinetic ion (GeFi) particle simulation scheme using electric field **E** and magnetic field **B** directly as field variables. Corresponding nonlinear gyrokinetic equations in terms of **E** and **B** are also derived. This new GeFi-E&B scheme is applicable for simulating plasma dynamics covering a broad frequency range and using a realistic electron-to-ion mass ratio. Simulation results are successfully benchmarked against analytical theories.

1. Introduction

In simulating plasma kinetic physics, fully kinetic (FK) particle-in-cell (PIC) schemes [1, 2] treat both electrons and ions as fully kinetic Vlasov particles. In the FK simulations, orbits of charged particle are, thus, resolved for dynamics with characteristic frequencies up to the electron cyclotron frequency, which is generally comparable to the electron plasma frequency. The fully kinetic particle computation, however, is time consuming for the general plasma system with vastly disparate temporal and spatial scales due to the small mass ratio between electrons and ions. More specifically, on one hand, it resolves the electron cyclotron frequency and the electron Larmor radius ρ_e and/or Debye length λ_d, and, on the other hand, it needs to cover the system size $>>$ the ion Larmor radius ρ_i and the Alfvén time scale of the system. Due to this wide range of scale separation, artificial ion-to-electron mass ratio m_i/m_e or limited system size are often employed in simulations in order to accommodate the available computing resources.

For physical problems of low-frequency nature with frequency $\omega << \Omega_i$, where Ω_i is the ion cyclotron frequency, and wavelength comparable with or larger than particle Larmor radius, one may employ reduced simulation models such as the gyrokinetic (GK) [3, 4] and drift kinetic (DK) models [5]. In the GK models, gyro-averaging is applied

to ion orbits so the physics of $\omega << \Omega_i$ can be solved with time interval $\Delta t >$ ion cyclotron period. Hybrid models [6, 7, 8], meanwhile, have been used to simulate the physics with $\omega <$ or $\sim \Omega_i$ and $k_\perp \rho_i \sim 1$, in which the fully kinetic Vlasov ion dynamics is retained but electrons are treated as a massless fluid. Here, $k_\perp$ is the perpendicular wave number.

In order to retain electron kinetic physics up to $\omega << |\Omega_e|$, where Ω_e is the electron gyrofrequency, a gyrokinetic electron and fully kinetic ion (GeFi) model [9] has also been developed. This GeFi scheme is applicable to problems with wave frequency up to $\omega >> \Omega_i$ but $<< |\Omega_e|$. In the GeFi scheme, more specifically, the electron dynamics is handled by the GK equations [10, 11, 12], and the ions are treated as FK particles. Such scheme is valid for $\omega/|\Omega_e| << 1$, the ratio of parallel-to-perpendicular wave number $|k_\parallel/k_\perp|^2 << 1$, $k_\perp \rho_e \sim 1$, and $\rho_e << L$, where L is the scale length of the background magnetic field. In addition to the removal of high-frequency electron gyro-motions, the high frequency electron plasma oscillation is also suppressed in the GeFi scheme. The GeFi scheme is, therefore, suitable for the dynamics in which the wave modes ranging from Alfvén waves to lower-hybrid/whistler waves must be handled on an equal footing; such as the physical processes associated with collisionless magnetic reconnection with a finite guide field [13, 14] and lower-hybrid waves in tokamak plasmas [15, 16, 17].

In the GK equations and simulations, one often employs the potentials ($\delta\Phi$, $\delta\mathbf{A}$) as field variables. Here, $\delta\Phi$ and $\delta\mathbf{A}$ are, respectively, the scalar and vector potentials. Poisson's equations are thus needed to solve for the potentials and, thereby, advance the dynamics. Such practices can, often, become computationally expensive and/or difficult for realistic, nonuniform geometries and multi-dimensional problems. Moreover, in the existing GeFi scheme [9], the compressional magnetic perturbation, $\delta B_\parallel$, is used as a field variable, and one needs to solve coupled Poisson's equations for $\delta\Phi$ and $\delta B_\parallel$, which further post potential computation challenges in the realistic simulations.

The purpose of this work is to develop a new GeFi particle simulation scheme that directly employs the electric field $\mathbf{E}$ and magnetic field $\mathbf{B}$ as field variables, and advances particles accordingly. Previously, electromagnetic fields have also been used in various hybrid codes [6, 18]. These hybrid models, nevertheless, assume the quasi-neutrality condition, and neglect the displacement current. Thus, no space-charge waves (e.g., the lower-hybrid waves) are included in the dynamics. Our present model, termed as GeFi-E&B, on the other hand, is developed to include the displacement current and electron polarization current systematically. Our new scheme, thus, could also have potential applications beyond the GeFi scheme specifically discussed here.

The outline of the manuscript is as follows. The theoretical formulation of this new GeFi-E&B scheme is described in Section 2. In Section 3, we present a benchmark of GeFi-E&B simulations against the analytical linear dispersion relations in a uniform plasma. Cold plasma approximation, for simplicity, is used in the benchmarking. Such benchmarking also helps to delineate the validity regime of the present scheme. Finally, summary and discussion are given in section 4. Derivation of the nonlinear GK equation in terms of $\mathbf{E}$ and $\mathbf{B}$, which can be used to advance the electrons, is given in Appendix

A.

2. Theoretical formulation

In order to delineate this GeFi-E&B scheme in a concise manner, let us consider the simplest limit of linear waves in a uniform plasma. Note that in the GeFi approximation, we assume $k_\parallel << k_\perp$, $\omega << |\Omega_e|$, and the high frequency electron plasma oscillation is suppressed. Thus, the ion dynamics is governed by the Vlasov equation, and advanced via the electromagnetic field, $\mathbf{E}$ and $\mathbf{B}$, in the usual way [1]. The electron dynamics is, however, governed by the nonlinear gyrokinetic equations (see Appendix A).

2.1. Equations for $\delta\mathbf{E}_\perp$

We start from the description of the field equations to determine the perturbed electric field $\delta\mathbf{E}$ and magnetic field $\delta\mathbf{B}$. First, let us consider $\delta\mathbf{E}_\perp$. From conservation of the electron perpendicular (to $\mathbf{B}_0$) momentum, we have

$$n_e q_e \delta\mathbf{E}_\perp = [\nabla\cdot\delta\mathbf{P_e}]_\perp - \delta\mathbf{J}_e\times\mathbf{B}_0/c + \frac{m_e}{q_e}\frac{\partial}{\partial t}\delta\mathbf{J}_{e\perp}. \tag{1}$$

Here, n_e is the unperturbed electron density, q_e is the electron change, $\delta\mathbf{J}_e$ is the perturbed electron current density, $\delta\mathbf{P_e} = m_e < \mathbf{vv}\delta f_e >_v$ is the perturbed electron pressure tensor, δf_e is the perturbed electron distribution function readily given by the gyrokinetic equations, Eqs. (A.1) and (A.17) (in Appendix A), and $< ... >_v$ denotes velocity-space integration. The rest of notations is standard.

For the GK electrons, it is more straightforward and accurate to calculate $\delta\mathbf{J}_e$ through

$$\delta\mathbf{J}_e = \delta\mathbf{J} - \delta\mathbf{J}_i. \tag{2}$$

From Maxwell's equation, we have

$$\delta\mathbf{J} = \frac{c}{4\pi}(\nabla\times\delta\mathbf{B}) - \frac{1}{4\pi}\frac{\partial}{\partial t}\delta\mathbf{E} \equiv \delta\mathbf{J}_B + \delta\mathbf{J}_d. \tag{3}$$

Note that $\delta\mathbf{J}_d$ corresponds to the displacement current and needs to be kept in order to properly account for the space-charge waves, e.g., the lower-hybrid waves.

In the interested limits of $|\omega/\Omega_e| << 1$ and $|\omega\Omega_e/\omega_{pe}^2| << 1$, where $\Omega_e = q_eB/m_ec$ is the electron cyclotron frequency and $\omega_{pe} = (4\pi n_e q_e^2/m_e)^{1/2}$ is the electron plasma frequency, we can readily demonstrate that Eq. (1) can be solved perturbatively as

$$\delta\mathbf{E}_\perp = \delta\mathbf{E}_{\perp 0} + \delta\mathbf{E}_{\perp p} + \delta\mathbf{E}_{\perp d}, \tag{4}$$

where

$$\delta\mathbf{E}_{\perp 0} = \left\{[\nabla\cdot\delta\mathbf{P_e}]_\perp - \delta\mathbf{J}_{e0}\times\mathbf{B}_0/c\right\}/n_eq_e, \tag{5}$$

$$\delta\mathbf{J}_{e0} = \delta\mathbf{J}_B - \delta\mathbf{J}_i, \tag{6}$$

$$\delta\mathbf{E}_{\perp p} = \frac{1}{n_eq_e^2}m_e\frac{\partial}{\partial t}\delta\mathbf{J}_{e\perp} \simeq \frac{m_e}{n_eq_e^2}\frac{\partial}{\partial t}\delta\mathbf{J}_{e0\perp}, \tag{7}$$

and

$$\delta \mathbf{E}_{\perp d} = -(\delta \mathbf{J}_d \times \mathbf{B}_0)/(cn_e q_e) \simeq \frac{1}{4\pi c n_e q_e} \frac{\partial}{\partial t} \delta \mathbf{E}_{\perp 0} \times \mathbf{B}_0. \tag{8}$$

Noting the $\partial/\partial t$ operator on $\delta \mathbf{E}_{\perp p}$ and $\delta \mathbf{E}_{\perp d}$, we may express $\delta \mathbf{E}_\perp$ finally as

$$\delta \mathbf{E}_\perp = \delta \mathbf{E}_{\perp 0} + \frac{\partial}{\partial t} \delta \hat{\mathbf{E}}_{\perp p} + \frac{\partial}{\partial t} \delta \hat{\mathbf{E}}_{\perp d}. \tag{9}$$

Here,

$$\delta \hat{\mathbf{E}}_{\perp p} = \frac{m_e}{n_e q_e^2} \delta \mathbf{J}_{e0\perp}, \tag{10}$$

and

$$\delta \hat{\mathbf{E}}_{\perp d} = \frac{1}{4\pi c n_e q_e} \delta \mathbf{E}_{\perp 0} \times \mathbf{B}_0. \tag{11}$$

2.2. Equations for $\delta \mathbf{E}_\parallel$

Next, let us consider $\delta \mathbf{E}_\parallel$. Taking $\partial/\partial t$ of Ampere's law, we have

$$c(\nabla \times \frac{\partial}{\partial t} \delta \mathbf{B}) = 4\pi \frac{\partial}{\partial t} \delta \mathbf{J} + \frac{\partial^2}{\partial t^2} \delta \mathbf{E}. \tag{12}$$

Applying Faraday's law, $\frac{\partial}{\partial t} \delta \mathbf{B} = -c \nabla \times \delta \mathbf{E}$, we have, for the parallel component and noting $|\frac{\partial^2}{\partial t^2}| << |c^2 \nabla_\perp^2|$,

$$c^2 [\nabla_\perp^2 \delta E_\parallel - \mathbf{b}_0 \cdot \nabla (\nabla \cdot \delta \mathbf{E}_\perp)] = 4\pi \frac{\partial}{\partial t} \delta J_\parallel. \tag{13}$$

Here, $\mathbf{b}_0 = \mathbf{B}_0/B_0$. For $m_e << m_i$, the parallel current is predominantly carried by electrons, i.e.,

$$\frac{\partial}{\partial t} \delta J_\parallel \simeq \frac{\partial}{\partial t} \delta J_{\parallel e}. \tag{14}$$

Noting the gyrokinetic equation for parallel momentum balance, Eqs. (A.24) in Appendix A, we have, in the linear and uniform plasma limit,

$$\frac{\partial}{\partial t} \delta J_{\parallel e} = -\frac{q_e}{m_e} \mathbf{b}_0 \cdot \nabla \delta P_{e\parallel} + \frac{n_0 q_e^2}{m_e} \Gamma_0 \delta E_\parallel - \frac{q_e}{m_e B_0} P_{e\perp 0} \Gamma_{0*} \mathbf{b}_0 \cdot \nabla \delta B_\parallel, \tag{15}$$

where $\delta P_{e\parallel} = m_e < v_\parallel^2 J_0 \delta F_{ge} >_v$, $n_0 \Gamma_0 =< F_{0e} J_0^2 >_v$, $P_{e\perp 0} \Gamma_{0*} = m_e < \frac{v_\perp^2}{2} F_{0e} J_0 J_{0*} >_v$, $J_0 = J_0(k_\perp \rho_e)$, $J_{0*} = J_0(k_\perp \rho_e/\sqrt{2})$, and $\rho_e = v_\perp/|\Omega_e|$. Inserting Eq. (15) into (13), we then arrive at the desired equation for $\delta E_\parallel$, i.e.,

$$(c^2 \nabla_\perp^2 - \omega_{pe}^2 \Gamma_0) \delta E_\parallel = -\mathbf{b}_0 \cdot \nabla [4\pi \frac{q_e}{m_e} (\delta P_{e\parallel} + \frac{P_{e\perp 0} \Gamma_{0*}}{B_0} \delta B_\parallel) - c^2 (\nabla \cdot \delta \mathbf{E}_{\perp 0})]. \tag{16}$$

Here, we have approximated $\nabla \cdot \delta \mathbf{E}_\perp \simeq \nabla \cdot \delta \mathbf{E}_{\perp 0}$.

2.3. Calculation of $\delta\mathbf{B}$

With $\delta\mathbf{E}$ determined, we can calculate $\delta\mathbf{B}$ from Faraday's law,

$$\frac{\partial}{\partial t}\delta\mathbf{B} = -c\nabla\times\delta\mathbf{E}. \tag{17}$$

Noting Eq. (9), Eq. (17) can be written as

$$\frac{\partial}{\partial t}\delta\mathbf{B} = -c\nabla\times(\delta\mathbf{E}_{\perp 0} + \frac{\partial}{\partial t}\delta\hat{\mathbf{E}}_{\perp p} + \frac{\partial}{\partial t}\delta\hat{\mathbf{E}}_{\perp d} + \delta\mathbf{E}_{\parallel}). \tag{18}$$

Defining

$$\delta\hat{\mathbf{B}} = \delta\mathbf{B} + c\nabla\times(\delta\hat{\mathbf{E}}_{\perp p} + \delta\hat{\mathbf{E}}_{\perp d}), \tag{19}$$

Eq. (17) becomes

$$\frac{\partial}{\partial t}\delta\hat{\mathbf{B}} = -c\nabla\times(\delta\mathbf{E}_{\perp 0} + \delta\mathbf{E}_{\parallel}). \tag{20}$$

Eq. (20) can then be used to advance $\delta\hat{\mathbf{B}}$.

Given $\delta\hat{\mathbf{B}}$, we need to apply Eq. (19) to solve for $\delta\mathbf{B}$; noting that both $\delta\hat{\mathbf{E}}_{\perp p}$ and $\delta\hat{\mathbf{E}}_{\perp d}$ depend on $\delta\mathbf{B}$ via $\delta\mathbf{J}_{e\perp 0}$ and $\delta\mathbf{E}_{\perp 0}$. Specifically, noting Eqs. (10) and (11) along with Eqs. (5) and (6), we can readily show that, after some straightforward algebra,

$$\delta\hat{\mathbf{E}}_{\perp p} + \delta\hat{\mathbf{E}}_{\perp d} = (\delta\hat{\mathbf{E}}_{dp} + \delta\hat{\mathbf{E}}_{i} + \delta\hat{\mathbf{E}}_{B}), \tag{21}$$

where

$$\delta\hat{\mathbf{E}}_{dp} = \frac{1}{4\pi c n_e^2 q_e^2}[\nabla\cdot\delta\mathbf{P_e}]_{\perp}\times\mathbf{B}_0, \tag{22}$$

$$\delta\hat{\mathbf{E}}_{i} = -\frac{4\pi}{\omega_{pe}^2}\hat{\epsilon}_{\perp}\delta\mathbf{J}_{i\perp}, \tag{23}$$

and

$$\delta\hat{\mathbf{E}}_{B} = \frac{4\pi}{\omega_{pe}^2}\hat{\epsilon}_{\perp}\delta\mathbf{J}_{B\perp}, \tag{24}$$

where

$$\hat{\epsilon}_{\perp} = 1 + \frac{\Omega_e^2}{\omega_{pe}^2}. \tag{25}$$

Noting $\delta\mathbf{J}_{B\perp} = \frac{c}{4\pi}(\nabla\times\delta\mathbf{B})_{\perp}$, we then have, neglecting self-consistently $O(k_{\parallel}^2/k_{\perp}^2)$ terms,

$$\nabla\times\delta\mathbf{J}_{B\perp} = \frac{c}{4\pi}[-\nabla_{\perp}^2\delta\mathbf{B}_{\parallel} + \nabla_{\perp}(\mathbf{b}_0\cdot\nabla\delta B_{\parallel})]. \tag{26}$$

Eq. (19) can then be expressed as

$$\delta\hat{\mathbf{B}} = \delta\mathbf{B} + c\nabla\times(\delta\hat{\mathbf{E}}_{dp} + \delta\hat{\mathbf{E}}_{i}) + d_e^2\hat{\epsilon}_{\perp}[-\nabla_{\perp}^2\delta\mathbf{B}_{\parallel} + \nabla_{\perp}(\mathbf{b}_0\cdot\nabla\delta B_{\parallel})], \tag{27}$$

where $d_e = c/\omega_{pe}$ is the electron skin depth. Taking components of Eq. (27), we have

$$(1 - \hat{\epsilon}_{\perp}d_e^2\nabla_{\perp}^2)\delta B_{\parallel} = \delta\hat{B}_{\parallel} - \mathbf{b}_0\cdot c\nabla\times(\delta\hat{\mathbf{E}}_{dp} + \delta\hat{\mathbf{E}}_{i}), \tag{28}$$

and

$$\delta\mathbf{B}_{\perp} = \delta\hat{\mathbf{B}}_{\perp} - c[\nabla\times(\delta\hat{\mathbf{E}}_{dp} + \delta\hat{\mathbf{E}}_{i})]_{\perp} - d_e^2\hat{\epsilon}_{\perp}\nabla_{\perp}(\mathbf{b}_0\cdot\nabla\delta B_{\parallel}). \tag{29}$$

Eqs. (28) and (29) then yield $\delta\mathbf{B}$. Noting that $\nabla\cdot\delta\hat{\mathbf{B}} = 0$, from Eqs. (20) and (27) readily yields $\nabla\cdot\delta\mathbf{B} = 0$.

3. Theoretical and numerical benchmark

In this section, we show a benchmark of the above GeFi-E&B formulation against the analytical dispersion relation in uniform plasma. For simplicity, let us consider the cold plasma limit in order to demonstrate that the present scheme contains both the electromagnetic and the electrostatic space-charge waves self-consistently, as well as to delineate its regime of validity.

Let the background magnetic field be $\mathbf{B}_0 = B_0\mathbf{e}_z$, so $\mathbf{b}_0 = \mathbf{e}_z$. The wave vector is assumed to be in the xz plane, with $\mathbf{k} = (k_\perp, 0, k_\parallel)$. Carrying out the tedious but straightforward analysis, we can then obtain the following GeFi-E&B linear dispersion relation for a cold and uniform plasma as

$$||A|| = 0, \tag{30}$$

where

$$\mathbf{A} = \begin{vmatrix} A_{11} & A_{12} & N_\perp N_\parallel \\ A_{21} & A_{22} & 0 \\ N_\perp N_\parallel & 0 & -(N_\perp^2 + \frac{\omega_{pe}^2}{\omega^2}) \end{vmatrix}, \tag{31}$$

$$A_{11} = -N_\parallel^2 + \frac{\omega_{pe}^2}{\Omega_e^2}\hat{\epsilon}_\perp\frac{N_\perp^2}{N^2} + (1 - \hat{\epsilon}_\perp k_\parallel^2 d_e^2)\frac{\omega_{pi}^2}{(\Omega_i^2 - \omega^2)}[1 + \frac{\Omega_i}{\Omega_e}\frac{N_\perp^2}{N^2}\hat{\epsilon}_\perp], \tag{32}$$

$$A_{12} = i\frac{\omega_{pe}^2}{\omega\Omega_e} + i\frac{\omega_{pi}^2\Omega_i}{\omega(\Omega_i^2 - \omega^2)}(1 - \hat{\epsilon}_\perp k_\parallel^2 d_e^2), \tag{33}$$

$$A_{21} = -A_{12} - i(1 - \hat{\epsilon}_\perp k_\parallel^2 d_e^2)\hat{\epsilon}_\perp\frac{N_\perp^2}{N^2}\frac{\omega_{pi}^2}{(\Omega_i^2 - \omega^2)}\frac{\omega}{\Omega_e}, \tag{34}$$

and

$$A_{22} = -N^2 + (1 - \hat{\epsilon}_\perp k_\parallel^2 d_e^2)\frac{\omega_{pi}^2}{(\Omega_i^2 - \omega^2)}. \tag{35}$$

Here, $\Omega_{i,e} = q_i B/m_{i,e}c$ carries the sign of charge , $\omega_{pi} = (4\pi n_e q_i^2/m_i)^{1/2}$, $N = kc/\omega$, $N_\parallel = k_\parallel c/\omega$, and $N_\perp = k_\perp c/\omega$.

To delineate its regime of validity, let us write the fully electromagnetic cold-plasma dispersion relation given, in the Stix notation [19], as

$$||\epsilon|| = 0, \tag{36}$$

where $\epsilon_{11} = -N_\parallel^2 + S$, $\epsilon_{12} = -\epsilon_{21} = -iD$, $\epsilon_{13} = \epsilon_{31} = N_\parallel N_\perp$, $\epsilon_{22} = -N^2 + S$, $\epsilon_{23} = \epsilon_{32} = 0$, $\epsilon_{33} = -N_\perp^2 + P$,

$$S = 1 + \frac{\omega_{pe}^2}{\Omega_e^2} + \frac{\omega_{pi}^2}{(\Omega_i^2 - \omega^2)}, \tag{37}$$

$$D = -[\frac{\omega_{pe}^2}{\omega\Omega_e} + \frac{\omega_{pi}^2\Omega_i}{\omega(\Omega_i^2 - \omega^2)}], \tag{38}$$

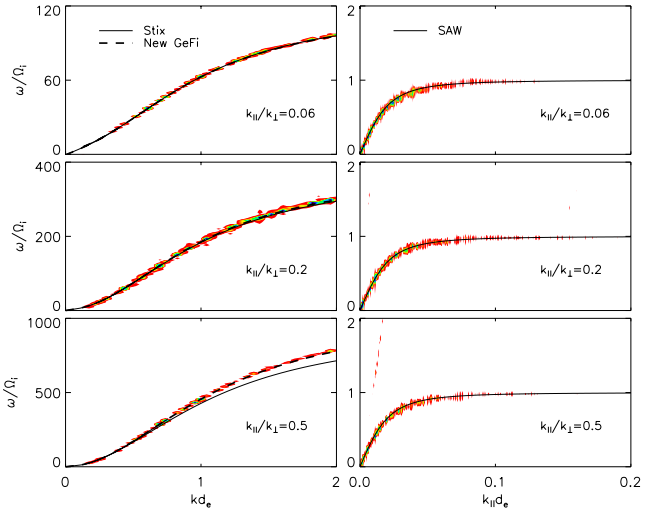

Figure 1. Linear dispersion relations of the high-frequency fast magnetosonic/whistler/lower-hybrid branch (left column) and the low-frequency shear Alfvén/ion cyclotron branch (right column), shown for $\delta B_\perp$ in cases with various $k_\parallel/k_\perp$, obtained from the numerical simulations based on the GeFi E&B scheme (color contours), the fully electromagnetic analytical theory (solid lines), and the GeFi E&B analytical theory (dashed lines).

and

$$P = 1 - \Sigma_{j=e,i} \frac{\omega_{pj}^2}{\omega^2}. \tag{39}$$

Comparison between ϵ and A clear demonstrates that the GeFi-E&B scheme is valid in the regime in which m_e/m_i, $\hat{\epsilon}_\perp k_\parallel^2 d_e^2$, $|\omega/\Omega_e|$, ω/ω_{pe}, $|k_\parallel/k|^2$, $|1/N^2| << 1$; consistent with the assumptions made in the formulation and derivations of the corresponding equations.

We have, furthermore, carried out direct numerical simulations in order to verify the numerical scheme and benchmark simulation results against analytical theories. Figure 1 shows a comparison among the linear dispersion relations obtained from the direct numerical simulations based on the present scheme (shown as the color contours in Figure 1), the fully electromagnetic analytical theory given by Eq. (36) (solid lines), and the GeFi E&B analytical theory given by Eq. (30) (dashed lines). Plotted in Figure 1 are the $\delta B_\perp$ component, with the left column for the high-frequency fast magnetosonic/whistler/lower-hybrid branch and the right column for the low-frequency shear Alfvén/ion cyclotron branch. The top, middle, and bottom rows in Figure 1 present the results of cases with $k_\parallel/k_\perp = 0.06$, 0.2, and 0.5, respectively. The linear fluctuations in the simulation data is generated from the random noise in a one-dimensional system. All results are based on $m_i/m_e = 1836$, $c/V_A = 400$, and thus $\omega_{pe}/\Omega_e = 9.35$. For the numerical simulations, the total number of ion particles per cell is 1000, with $\beta_i = 4 \times 10^{-6}$, whereas the electrons are assumed to be cold. It is seen from Figure 1 that the GeFi-E&B simulation results agree very well with those from the GeFi-E&B analytical dispersion relation for various $k_\parallel/k_\perp$. Moreover, these GeFi-E&B

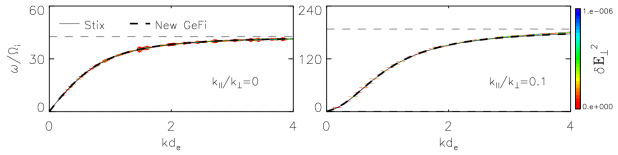

Figure 2. Comparison between the simulation results (color contours) and the fully electromagnetic analytical linear dispersion relation (dashed line), both based on the GeFi-E&B scheme, for the $\delta E_\perp$ component in cases with $k_\parallel/k_\perp = 0$ (left plot) and 0.1 (right). The cold plasma electrostatic dispersion relation is recovered at the $k_\perp^2 d_e^2 >> 1$ limit.

results also agree very well with Stix's fully electromagnetic results for $k_\parallel/k_\perp = 0.06$ and 0.2. The deviation increases with increasing $k_\parallel/k_\perp$, or ω/Ω_e, as expected for the GeFi-E&B validity regime. Nevertheless, the deviation is less than 10% for $k_\parallel/k_\perp = 0.5$.

To demonstrate that the present scheme describes accurately the electrostatic space-charge waves, Figure 2 compares the GeFi-E&B numerical results (color contours) with the fully electromagnetic analytical linear dispersion relation (dashed line) for $\delta E_\perp$ in cases with $k_\parallel/k_\perp = 0$ (left plot) and 0.1 (right plot). Taking the $k_\perp^2 d_e^2 >> 1$ limit, we readily have the following cold plasma electrostatic dispersion relation

$$1 + \frac{\omega_{pe}^2}{\Omega_e^2} - \frac{\omega_{pi}^2}{(\Omega_i^2 - \omega^2)} \simeq \frac{k_\parallel^2}{k_\perp^2}\frac{\omega_{pe}^2}{\omega^2}, \tag{40}$$

and the results are plotted as the dashed lines in Figure 2. It can be clearly seen from Figure 2 that the analytical electrostatic solutions are well recovered in our GeFi-E&B simulation results in the appropriate asymptotic limit of $k_\perp^2 d_e^2 >> 1$.

4. Summary and discussion

In summary, a GeFi-E&B scheme has been developed to implement the GeFi particle simulation model with the electromagnetic fields, **E** and **B**, as field variables directly. Contrary to previous hybrid models that also employ the electromagnetic fields, the quasi-neutrality condition is not assumed in the present GeFi-E&B model. Furthermore, the displacement current and electron polarization current are retained systematically in the calculations, and, thus, the space-charge waves are self-consistently included in the dynamics. In addition, nonlinear gyrokinetic equations in terms of **E** and **B** have also been derived.

The new scheme has been successfully benchmarked for cold plasma waves in uniform plasma. The validity regime of the scheme has been demonstrated as m_e/m_i, $|k_\parallel^2/k_\perp^2|$, $|\omega/\Omega_e|$, $|\omega/\omega_{pe}|$, $k_\parallel^2 d_e^2 << 1$, and $N^2 = (ck/\omega)^2 >> 1$; similar to that in the original GeFi scheme based on Φ and **A** [9]. The GeFi schemes, therefore, can adopt a realistic small mass ratio of m_e/m_i to study physics issues covering a broad frequency range of interest for space and laboratory plasmas.

The GeFi-E&B scheme has computational advantage because it does not heavily involve solving the Poisson's equations as the original GeFi scheme [9] does. Although

our focus of this work is on the gyrokinetic electrons and fully kinetic ion description, our GeFi E&B scheme also has potential applications beyond the GeFi approach. The field solving scheme, more specifically, can be used for other models of electron and/or ion dynamics; e.g., with the fluid approximation.

Finally, it is noted that in the current work, we present the GeFi-E&B model in the linear and uniform plasma limit in order to illustrate clearly the scheme and its theoretical foundation. Obviously, for practical applications, the scheme needs to be extended to the general nonuniform and nonlinear cases. One can readily recognize that while the detailed algebra becomes tedious for the general system, the conceptual formulation is rather straightforward. The extended formulation and its analysis will be reported in a future publication.

Acknowledgments

This work was supported by DoE grant DE-SC0018071 to Auburn University, grant No.11235009 of the National Science Foundation of China, and the ITER-CN project. Computer resources were provided by the Alabama Supercomputer Center.

Appendix A. Derivation of nonlinear gyrokinetic equations in E & B fields

In this appendix, we derive the gyrokinetic equation in the **E** and **B** fields. Following the Frieman and Chen [10] nonlinear gyrokinetic equation and assuming an isotropic equilibrium distribution function for now, we can show [18]

$$f = \delta f_{pol} + T_g^{-1}(F_g), \tag{A.1}$$

where

$$\delta f_{pol} = \frac{q}{m}[\delta\phi - T_g^{-1} < \delta\phi >]\frac{\partial F_0}{\partial \epsilon}, \tag{A.2}$$

$\delta\phi$ is the perturbed electrostatic potential, $\epsilon = v^2/2$, $T_g = \exp(\rho \cdot \nabla_\perp)$, $\rho = \mathbf{b}_0 \times \mathbf{v}/\Omega$, $\mathbf{b}_0 = \mathbf{B}_0/B_0$, $\Omega = qB_0/mc$, and $< ... >$ denotes averaging over the gyro angle. F_g, meanwhile, satisfies

$$[\frac{\partial}{\partial t} + \dot{\mathbf{R}} \cdot \nabla + \dot{\epsilon}\frac{\partial}{\partial \epsilon}]F_g(\mathbf{R}, \mu, t) = 0. \tag{A.3}$$

Here, $\mu = v_\perp^2/2B_0$,

$$\dot{\mathbf{R}} = \dot{\mathbf{R}}_0 + < \delta\mathbf{u}_g >, \tag{A.4}$$

$$\dot{\mathbf{R}}_0 = v_\parallel \mathbf{b}_0 + \mathbf{V}_{dB} + \mathbf{V}_{dK}, \tag{A.5}$$

$$\mathbf{V}_{dB} = \frac{\mu}{\Omega}\mathbf{b}_0 \times \nabla B_0, \tag{A.6}$$

$$\mathbf{V}_{dK} = \frac{v_\parallel^2}{\Omega}\mathbf{b}_0 \times \kappa, \tag{A.7}$$

and $\kappa = \mathbf{b}_0 \cdot \nabla \mathbf{b}_0$ is the curvature of $\mathbf{B}_0$. Meanwhile,

$$< \delta \mathbf{u}_g > = < \delta \mathbf{u}_E > + < \delta \mathbf{u}_{B\perp} > + < \delta \mathbf{u}_{B\parallel} > \tag{A.8}$$

is the gyro-averaged perturbed guiding-center velocity,

$$< \delta \mathbf{u}_E > = \frac{c}{B_0} < \delta \mathbf{E}_\perp > \times \mathbf{b}_0, \tag{A.9}$$

$$< \delta \mathbf{u}_{B\perp} > = v_\parallel < \delta \mathbf{B}_\perp > / \mathbf{B}_0, \tag{A.10}$$

$$< \delta \mathbf{u}_{B\parallel} > = -\frac{1}{B_0} \mathbf{b}_0 \times \nabla_\perp < \mathbf{v}_\perp \cdot \delta \mathbf{A}_\perp >, \tag{A.11}$$

and $< \mathbf{A} > = J_0(k_\perp \rho)\mathbf{A}$. Noting that [20]

$$< \frac{\mathbf{v}_\perp \cdot \delta \mathbf{A}_\perp}{c} > = -\frac{v_\perp J_1}{k_\perp c} \delta B_\parallel \tag{A.12}$$

and matching accuracy to $O(k_\perp^2 \rho^2)$, we may approximately write

$$< \frac{\mathbf{v}_\perp \cdot \delta \mathbf{A}_\perp}{c} > \simeq -\frac{m}{q} \mu J_0(\frac{k_\perp \rho}{\sqrt{2}}) \delta B_\parallel \equiv -\frac{m}{q} \mu < \delta B_\parallel >_* . \tag{A.13}$$

Thus, $< ... >_*$ denotes gyro-phase averaging at an effective Larmor radius of $\rho/\sqrt{2}$ [21]. Thus, Eq. (A.11) becomes

$$< \delta \mathbf{u}_{B\parallel} > = \frac{\mu}{\Omega} \mathbf{b}_0 \times \nabla < \delta B_\parallel >_* . \tag{A.14}$$

$\dot{\epsilon}$, meanwhile, is given by

$$\dot{\epsilon} = -\frac{q}{m} \dot{\mathbf{R}} \cdot \nabla < \delta \phi > - \frac{q}{m} \frac{\partial}{\partial t} < \frac{\mathbf{v} \cdot \delta \mathbf{A}}{c} > . \tag{A.15}$$

Within the gyrokinetic ordering $|\frac{\partial}{\partial t}|/|\mathbf{v}_\perp \cdot \nabla_\perp| \sim O(\epsilon) << 1$, we have $\delta \mathbf{E}_\perp = -\nabla_\perp \delta \phi$. Eq. (A.15) can then be written as

$$\dot{\epsilon} = \frac{q}{m} [\dot{\mathbf{R}} \cdot < \delta \mathbf{E}_\perp > + v_\parallel < \delta E_\parallel >] + \mu \frac{\partial}{\partial t} < \delta B_\parallel >_* . \tag{A.16}$$

We can now transform from the ϵ to $v_\parallel$ phase space. It is then straightforward to derive the following nonlinear gyrokineitc equation for $F_g(\mathbf{R}, v_\parallel, \mu, t)$,

$$[\frac{\partial}{\partial t} + \dot{\mathbf{R}} \cdot \nabla + \dot{v}_\parallel \frac{\partial}{\partial v_\parallel}] F_g = 0, \tag{A.17}$$

where $\dot{\mathbf{R}}$ is given by Eq. (A.4), and

$$\dot{v}_\parallel = \dot{\mathbf{R}} \cdot \nabla v_\parallel + \frac{\dot{\epsilon}}{v_\parallel} = \mathbf{b}_* \cdot [\frac{q}{m} < \delta \mathbf{E} > - \mu \nabla B], \tag{A.18}$$

$$\mathbf{b}_* = \mathbf{b}_0 + \frac{v_\parallel}{\Omega} \mathbf{b}_0 \times \kappa + \frac{< \delta \mathbf{B}_\perp >}{B_0}, \tag{A.19}$$

and

$$B = B_0 + < \delta B_\parallel >_* . \tag{A.20}$$

Note that the polarization contribution, δf_{pol} of Eq. (A.2) can be expressed as

$$< \delta f_{pol} > = \frac{q}{m} [1 - J_0(k_\perp \rho)^2] \delta \phi \frac{\partial F_0}{\partial \epsilon}, \tag{A.21}$$

which, for $|k_\perp\rho|^2 < 1$, can be approximately expressed as

$$< \delta f_{pol} > \simeq \frac{q}{m}\nabla_\perp \cdot \frac{\rho^2}{2}\frac{\partial F_0}{\partial \epsilon}\delta \mathbf{E}_\perp. \tag{A.22}$$

If necessary, we may employ Pade's approximation to derive $< \delta f_{pol} >$ for arbitrary $k_\perp\rho$ as

$$(1 - \frac{\rho}{2}\nabla_\perp^2) < \delta f_{pol} > \simeq \frac{q}{m}\nabla_\perp \cdot \frac{\rho^2}{2}\frac{\partial F_0}{\partial \epsilon}\delta \mathbf{E}_\perp. \tag{A.23}$$

Eqs. (A.1) and (A.17) along with Eq. (A.22) or (A.23) then provide a complete nonlinear gyrokinetic equation in terms of $\delta\mathbf{E}$ and $\delta\mathbf{B}$.

With f given by Eq. (A.1) along with Eq. (A.17) , we can then calculate density, $n = \int d^3v = \int d\alpha B_0 d\mu dv_\parallel f \equiv < f >_v$, with α being the gyrophase angle and the pressure tensor $P = m < \mathbf{v}\mathbf{v}f >_v$. In particular, we may derive the following gyrokinetic parallel momentum balance equation

$$\begin{aligned} &\frac{\partial}{\partial t}J_\parallel = -\frac{q}{m}\mathbf{b}_0 \cdot \nabla P_{g\parallel} - q < (\mathbf{V}_{dB} + \mathbf{V}_{dK}) \cdot \nabla (v_\parallel J_0 F_g) >_v \\ &-q < J_0[< \delta \mathbf{u}_g > \cdot \nabla (v_\parallel F_g)] >_v \\ &+\frac{q}{m} < J_0[(\mathbf{b} + 2\frac{v_\parallel}{\Omega}\mathbf{b}_0 \times \kappa)F_g \cdot (\frac{q}{m} < \delta \mathbf{E} > -\mu \nabla B)] >_v, \end{aligned} \tag{A.24}$$

where $\mathbf{b} = \mathbf{b}_0 + < \delta \mathbf{B}_\perp > /B_0$.

Finally, we note that, in the $|k_\perp\rho|^2 << 1$ limit, we have T_g, $J_0 \simeq 1$ and $f \simeq F_g$, Eq. (A.17) then reduces to the well-known drift-kinetic equation, as it should. The corresponding parallel momentum balance equation, meanwhile, becomes, from Eq. (A.24),

$$\frac{\partial}{\partial t}J_\parallel = \mathbf{b}\cdot\frac{q}{m}(nq\mathbf{E} - \nabla P_{g\parallel} - \frac{P_{g\perp}}{B_0}\nabla B) - q < (\delta \mathbf{u}_{B\parallel} + \delta \mathbf{u}_E)\cdot\nabla(v_\parallel F_g) >_v . \tag{A.25}$$

Here, $P_{g\perp} = m < (v_\perp^2/2)F_g >$, $\delta \mathbf{u}_E = c\delta \mathbf{E}_\perp \times \mathbf{b}_0/B_0$, and $\delta \mathbf{u}_{B\parallel} = (\mu/\Omega)\mathbf{b}_0 \times \nabla \delta B_\parallel$.

References

[1] Birdsall C K and Langdon A B 2004 *Plasma physics via computer simulation* (CRC Press) pp. 11-15
[2] Dawson John M 1983 *Rev. Mod. Phys.* **55** 403
[3] Lee W W 1983 *Phys. Fluids* **26** 556
[4] Lee W W 1987 *J. Comput. Phys.* **72** 243
[5] Hazeltine R D 1973 *Plasma Physics* **15** 77
[6] Swift D W and Lee L C 1983 *J. Geophys. Res.* **88** 111
[7] Winske D and Quest K B 1986 *J. Geophys. Res.* **91** 8789
[8] Lin Y, Wang X Y, Lu S, Perez J D, and Lu Q 2014 *J. Geophys. Res. Space Phys.* **119** 7413
[9] Lin Y, Wang X Y, Lin Z and Chen L 2005 *Plasma Phys. Control. Fusion* **47** 657
[10] Frieman E A and Chen L 1982 *Phys. Fluids* **25** 502
[11] Hahm T S, Lee W W and Brizard A 1988 *Phys. Fluids* **31** 1940
[12] Brizard A 1989 *J. Plasma Phys.* **41** 541
[13] Wang X Y, Lin Y, Chen L, Lu X, and Kong W 2011 *Phys. Plasmas* **18** 122102
[14] Wang Z, Lin Y, Wang X Y, Tummel K, and Chen L 2016 *Phys. Plasmas* **23** 072104
[15] Qi L, Wang X Y, and Lin Y 2013 *Phys. Plasmas* **20** 062107

[16] Bao J, Lin Z, Kuley A, and Lu Z X 2014 *Plasma Phys. Control. Fusion* **56** 095020
[17] Jia G, Xiang N, Wang X Y, Huang Y, and Lin Y 2016 *Phys. Plasmas* **23** 012504
[18] Chen Y, and Parker S E 2009 *Phys. Plasmas* **16** 052305
[19] Stix T H 1992 *Waves in Plasmas* (American Institute of Physics, New York) pp. 237-264
[20] Antonsen T M, and Lane B 1980 *Phys. Fluids* **23** 1205
[21] Porazik P, and Lin Z 2011 *Comm. Comput. Phys.* **10** 899